Published in final edited form as:
Circulation. 2010 February 16; 121(6): 768–774. doi:10.1161/CIRCULATIONAHA.109.918151.

Extensible Behavior of Titin in the Miniswine Left Ventricle

Martin M. LeWinter, M.D.[1], **Joseph Popper, B.S.**[2], **Mark McNabb, B.S.**[2], **Lori Nyland, M.S.**[1], **Stephen B. Bell, B.S.**[1], and **Henk Granzier, Ph.D.**[2]

[1] Cardiology Unit, University of Vermont College of Medicine

[2] Department of Molecular and Cellular Biology and Molecular Cardiovascular Research Program, University of Arizona

Abstract

Background—The sarcomeric protein titin is a molecular spring responsible for passive tension and restoring forces of cardiomyocytes. Extension of titin as a function of sarcomere length (SL) has been studied in rodents, who predominantly express the smaller, stiffer N2B titin isoform. Large mammals co-express roughly equal proportions of N2B and N2BA titin, the larger, more compliant isoform. We hypothesized that extension of titin in relation to SL differs in large mammals and this difference is functionally important.

Methods and Results—We characterized the filling pressure (FP)-SL relation in diastolic arrested miniswine LVs. SL was 2.15–2.25 μm at FP ~0 mmHg and reached a maximum of ~2.50 μm with overfilling. Over the normal FP range, SL ranged from ~2.32 to ~2.40 μm. We assessed titin extension as a function of SL using immunoelectron microscopy, which allowed delineation of the behavior of specific spring segments. The major isoform difference was that the N2B-Us segment extended ~4-fold more as a function of SL in N2B compared with N2BA titin. Using this segment we estimated sarcomeric force development with a worm-like chain model and found that N2B develops markedly greater force than N2BA titin. The resulting force with co-expression of N2B and N2BA titin is intermediate.

Conclusions—In light of murine studies showing that operating SLs are shorter than in miniswine, our results indicate that co-expression of the two titin isoforms in large mammals allows longer SLs without development of excessive diastolic tension.

Keywords

diastole; myocardium; ventricles; titin

Introduction

The giant sarcomeric protein titin is anchored in the Z-disc and bound to the thick filament.[1] Its I-band region contains a molecular spring consisting of PEVK, Ig repeat and N2B and N2A elements. In slack cardiomyoyctes the spring corresponds to a flexible chain with a mean square end-to-end distance much below its contour length (CL).[2] With lengthening, spring elements extend and passive tension develops.[3].[4] Over the physiologic sarcomere length (SL) range, titin is the predominant source of cardiomyocyte passive tension. In the normal left ventricle (LV) it contributes at least as much as collagen to passive myocardial stiffness.[5,6] At systolic

Corresponding Author: Martin M. LeWinter, M.D., Cardiology Unit, Fletcher Allen Health Care, 111 Colchester Ave., Burlington, VT 05401, FAX: 802 847-3637, Telephone: 802 847-2879, martin.lewinter@vtmednet.org.

Disclosures
No conflicts of interest.

SLs below slack, titin is an important source of the restoring force resulting in cardiomyocyte elastic recoil.[7]

In rodent LV, immuno electronmicroscopic (IEM) studies reveal that with sarcomere extension the spring elements of titin lengthen differentially, with each dominating distinct portions of the cardiomyocyte length-tension relation.[3,4] N2B titin, which contains the N2B but not the N2A element, predominates in rodent LV.[8] In contrast, large mammals including humans express mixtures of the N2BA isoform, containing both N2B and N2A elements, and the N2B isoform.[8–11] Both isoforms are co-expressed within the sarcomere.[12] Because N2B titin is much stiffer than N2BA titin, the passive stiffness of rodent cardiomyocytes, myocardium and LV exceeds that of large mammals.[8,9] Titin isoform switching (increased N2BA:N2B ratio) is observed in patients with dilated cardiomyopathy.[10,11] Moreover, considering the importance of clinical diastolic dysfunction[13], detailed information about how titin determines diastolic stiffness in large mammalian LVs is important to our understanding of heart failure.

In view of these isoform and stiffness differences, we hypothesized that SL range and titin behavior differ in large mammalian LVs compared with predominantly N2B expressing species and that these differences serve a useful function. Accordingly, in the present study we determined relations between transmural filling pressure (FP) and normalized diastolic segment length and SL in the intact miniswine LV arrested in diastole. Because turgor influences the LV FP-volume relation[14] experiments were performed with and without a physiologic level of coronary perfusion pressure (CPP). We then employed immuno electronmicroscopy to characterize extension of titin's spring elements and related these to SL and LV filling.

Methods

LV Filling Pressure-Sarcomere Length Relations

Protocol—11 male Yorkshire miniswine, average 28.4 kg (range 26–33), were used to delineate the LV transmural FP-SL relation over a range between ~0 mmHg and markedly over-distended conditions. They were sedated with ketamine (20 mg/kg im), anesthetized with isoflurane, and endotracheally intubated. Anesthesia was maintained with 2–3% isoflurane. A large animal respirator was used for ventilation with 100% supplemental oxygen. A midline sternotomy was performed, the pericardium incised, and the heart suspended in a pericardial cradle. Ascending aortic pressure was measured through a fluid-filled catheter inserted from a femoral artery. A 14F, fluid-filled, stiff plastic cannula with multiple sideholes was inserted in the LV through the apex and secured with a purse-string suture. LV pressure was measured through the cannula with a Becton Dickinson DTX Plus (DT-4812) transducer zeroed at the mid-right atrium. A pair of ultrasonic crystals (1.0 mm diameter) was then inserted ~ 1 cm apart to track motion of a circumferentially-oriented midwall segment in the LV anterior free wall at the level of its minor axis.[15] Midwall fibers at this site are oriented circumferentially in multiple species.[16–20] After completion of the experiments we confirmed that the crystals were midwall. Finally, inflatable cuffs were positioned around each caval vessel.

Once instrumentation was complete, warmed saline was administered intravenously as necessary to raise LV end-diastolic pressure (EDP) to the normal range (5–13 mmHg). Ventilation was then suspended at end-expiration, steady state-measurements of LV pressure and segment length were recorded for several beats and a bicaval occlusion was performed. The occlusion was maintained until LVEDP reached a minimum value.

Heparin sulfate 10,000 U i.v. was then administered, the azygous vein was ligated, and snares were positioned around the pulmonary hila and veins, caval vessels, and the aorta just above the aortic valve. The ultrasonic crystals were left in place. The heart was then arrested in diastole

with an aortic root injection of 35 ml of 20% KCL with 3mM butanedioxone monoxime and all snares secured in order to isolate the heart from the rest of the circulation. A plastic cannula was inserted into the free wall of the right ventricle, which was vented to atmosphere. The isolated left heart was drained of blood by applying negative pressure through the LV cannula.

We then filled the LV by re-infusing warmed (37°C), heparinized blood to a predetermined level of pressure encompassing a range from ~0 to ~50 mmHg. In 5 of the 11 experiments, CPP was not varied after arrest. Aortic pressure was in the 5–15 mmHg range under these conditions. In the other 6 experiments CPP was manipulated to a physiologic level. To accomplish this, after the arrested LV was filled to the desired pressure saline (37°C) was continuously infused into the aortic root below the snare at pressures ranging from 75 to 90 mmHg. Consistent with turgor[14], pressurizing the coronary circulation invariably raised the LV pressure, which was then lowered to the desired level by removal of blood. The increase in pressure with coronary pressurization was dependent on the starting LV pressure. It was 1–2 mmHg when the initial pressure was zero or near zero mmHg to > 10 mmHg in the heart with the highest pressure (~50 mmHg).

Once the desired FP was reached the heart was rapidly fixed by injecting 100 ml of 6.25% glutaraldehyde in phosphate buffer (pH 7.4) at 40ml/sec into the aortic root with a power injector during continuous recording with a General Electric OEC900 digital fluoroscopic. The glutaraldehyde injectate contained a small volume of radiographic contrast medium, which allowed us to verify that the aortic valve remained competent during fixation. By visualizing the radio-opaque ultrasonic crystals we determined that fixation did not change the distance between them. The ultrasonic crystal signal was monitored after cardiac arrest until the moment of fixation. Fixation resulted in an abrupt, upward shift of the signal. Because the directly visualized distance between the crystals did not change, it is likely that slowing of the speed of ultrasound by fixation caused this effect. After fixation an additional 50–100 ml of glutaraldehyde was flushed through the coronary circulation. The LV cannula and ultrasonic crystals were removed and the fixed heart removed from the chest and immersed in 6.25 % glutaraldehyde in phosphate buffer for ~24 hours at room temperature.

In order to measure SL at the smallest possible LV volume, one additional experiment was performed, without coronary pressurization. The LV was emptied by suction after cardiac arrest, the proximal left anterior descending coronary artery was cannulated, and the anterior wall selectively fixed by injecting glutaraldehyde directly into the vessel. We selectively fixed the anterior wall because in preliminary attempts we found that the aortic valve was incompetent during glutaraldehyde injection into the aortic root when the LV was fully collapsed. This heart was also immersed in glutaraldehyde overnight.

SL Measurement—On the following day, transmural sections (~1 cm^3) were removed from the fixed LV at the site where the crystals were inserted and washed in PBS. Thin strips ~ 2 mm long were dissected from the middle 1–2 mm of the wall, taking care to avoid straining the tissue and utilizing naturally occurring bundles of cardiomyocytes oriented in the same direction that were easy to separate from adjacent tissue. The strips were placed in a chamber with a glass bottom and top and average SL was measured by laser diffraction (~15 strips/heart).[21] Thus, each heart yielded one SL – EDP data point. Variation in SL amongst the strips from each heart was < 10 nm.

Data Analysis—SLs and associated FPs were fitted to a monoexponential function for conditions with and without coronary perfusion. In addition, the relation between normalized diastolic segment length change and SL was estimated. For this analysis, we used LVEDP – segment length data obtained during bicaval occlusion, as follows. During bicaval occlusion, minimum EDP usually reached values very near 0 mmHg. However, in two instances the

minimum value was in the 1–2 mm Hg range. Normalized diastolic segment length change for each heart was calculated as the segment length present just before fixation normalized to the value closest to 2 mmHg during bicaval occlusion (thus, values with EDP < 2 mmHg were <1). In two hearts, values could not be calculated because crystal tracking was lost at very low LVEDPs.

In addition to SL measured in the arrested heart, we calculated minimum systolic SLs during bicaval occlusion. To accomplish this, we matched the segment length present just before fixation to the SL measured in the midwall after fixation at the site of crystal placement. We assumed a linear relation between segment length and SL to calculate minimum systolic SL. As with normalized segment lengths, two hearts could not be used because of loss of crystal tracking.

Immunoelectron Microscopic Determination of Titin Extension—Because fixation precluded IEM measurements, we used four additional KCl arrested, unfixed hearts to dissect midwall strips (~10 mm length × 1 mm diameter, ~ 10 strips/heart) at the same site where crystals were inserted in the previous experiments. Strips were placed in relaxing solution with Triton for 8 hours, washed with relaxing solution and then stretched at ~0.1 μm/sarcomere to different lengths, where they were held, fixed in 3% formaldehyde/PBS solution, and washed and blocked in 1% BSA/PBS solution.[12] They were then immuno-labeled, embedded and processed for EM.[12] Antibodies were obtained from Eurogentec (Brussels, Belgium) and Biogenes (Berlin, Germany) and affinity purified. Titin monoconal antibody T12 was purchased from Boehringer-Mannheim (Indianapolis, IN). After dilution of antibodies to appropriate concentrations (typically ~50 μg/ml), samples were first labeled with primary and then secondary antibodies for 48 hours. Tissue was then fixed in 3% glutaraldehyde/0.2% tannic acid and 1% osmium-tetroxide solutions and embedded in araldite. Samples were dehydrated in graded series of ethanol, with final rinses in 100% propylene oxide prior to infiltration and embedding. Sections were cut using a Leica microtome and stained with 2% potassium permanganate and then 0.25% lead citrate. Images were obtained with a JEOL 1200 microscope. Z-line to epitope distances were measured from negatives following high-resolution scanning (UMAX, UC-1260) and digital image processing using custom written macros for the analysis program NIH Image (v. 1.6, Wayne Rasband, National Institutes of Health. This entire procedure yielded approximately 40 data points (10 strips × 4 hearts) at varying SLs per epitope. For additional details, see Trombitas et al.[12]

Statistics—Data are reported as mean ± SD. To test for slope and intercept differences between the FP-SL relations with and without physiologic CPP, a natural logarithm (ln) transformation of the SL data was performed to linearize pressure versus SL data based on their hypothesized exponential relationship. Transformed data were subjected to a General Linear Model analysis to examine the relationship of ln SL with pressure and to test the equality of slopes between high and low CPP groups using a group by pressure statistical interaction term. A subsequent nested model was used to test for equality of intercepts between the groups after accepting the equality of the slopes.[22]

Results

LV Filling Pressure – SL Relations

Relations between FP and anterior midwall SLs determined in the fixed LV are depicted in Figure 1 (top) for studies with (high CP) and without (low CP) coronary pressurization, along with fitted relations for each condition. A curvilinear relation is evident with and without coronary pressurization. The fitted relation appears shifted upward and to the left with coronary pressurization at filling pressures greater than 4–5 mmHg, again consistent with turgor.

Although in each case LV pressure rose with coronary pressurization at constant LV volume, neither slope nor intercept of the curves was significantly different at $p < .05$.

At FPs of ~ 0 mmHg, anterior midwall SL was in the 2.15 – 2.25 μm range. Because the slope of the relation is so flat over this range, it is difficult to be precise about SL at 0 mmHg. In the completely collapsed LV, SL was 1.99 μm. Thus, the true SL at 0 mmHg must be greater than this value. At FPs near the lower limit of normal (~ 5 mmHg), anterior midwall SL was in the 2.30–2.35 μm range. At the upper end of the normal range (12–13 mmHg), based on coronary pressurization data, SL was in the 2.45 μm range. At pressures greater than the normal range, SLs increased to a maximal of ~2.50 μm. The relation between normalized diastolic segment length change and SL is shown in the bottom of Figure 1. This relation was linear and, in contrast to filling pressure – SL relations, did not appear altered by coronary pressurization.

Typical recordings of LV pressure and segment length during bicaval occlusion are shown in Figure 2 (segment length is converted to SL, as described earlier). Baseline minimum systolic SL (the first three beats) was 1.90–1.95 μm. For the entire group, this value was 1.96 ± .16 μm. During bicaval occlusion minimum systolic SL progressively declined. The arrow indicates the first beat with estimated SL <1.85 μm; EDP was ~5 mmHg. The shortest SL in this example was ~1.65 μm, when EDP was ~ 1 mmHg. The lowest EDP during bicaval occlusion averaged 0.8 ± 1.2 mmHg for the entire group. Minimum systolic SL at this EDP was 1.68 ± 0.14 μm. In all but one experiment, minimum systolic SL at the lowest EDP was less than ~1.85–1.90 μm. By interpolating between data points for the eight experiments where SL was < 1.85 μm, we estimate that a SL of 1.85 μm was reached at EDPs ranging from 3–7 mmHg during bicaval occlusion.

Titin Extension by IEM

To delineate the extensibility of titin's spring elements we stretched skinned strips to various SLs encompassing the range determined in the FP-SL experiments and then immuno-labeled with antibodies to various epitopes, as shown in Fig. 3, left. Examples of labeled sarcomeres are shown in Fig. 3, right. Each antibody was detected in a single epitope per half sarcomere except for Uc, which is directed toward an epitope C-terminal of the N2B unique sequence and labels two epitopes per half sarcomere. We previously showed that the N2BA isoform is labeled closer to the Z-disk (due to extra extensibility provided by its middle tandem Ig and longer PEVK), whereas the N2B isoform labels closer to the A-band.[12] The epitope to mid Z-disk distance is plotted as a function of SL in Fig. 4, top (segments demarcated by the epitopes shown in Fig. 3, left). End-to-end lengths of the N2B-unique sequence (N2B-Us) are shown in Fig. 4, bottom. The lines of the linear fits indicate that N2B-Us extends ~4-fold more as a function of SL in the N2B than in the N2BA isoform.

Discussion

Sarcomere Lengths and Filling Pressure

In the present study we first delineated the relation between transmural FP and SL in the anterior midwall of the in situ, diastolic-arrested LV. At transmural FP ~ 0 mmHg, SLs were 2.15 – 2.25 μm. Because the filling pressure-SL relation is so flat around 0 mmHg we cannot be more precise about this value, but the SL of 1.99 μm in the collapsed LV establishes an approximate lower limit. In the closed-chest state the normal LV intra-cavitary FP is between about 5 and 12–13 mmHg. SLs were ~2.30 to ~ 2.45 μm over this range of FP. However, these values for the normal *intra-cavitary* FP range slightly overestimate transmural FP because they do not include the external pressure imposed on the LV by the pericardium. Under completely physiologic conditions with pericardium intact, at any intra-cavitary FP SL would be lower than that measured under the conditions of our experiments. We previously found that the intact

pericardium accounts for ~2 mmHg at a measured LV intra-cavitary pressure of ~12–13 mmHg.[23] Thus, in our experiments the upper limit of normal SL is best approximated by that present under conditions of coronary pressurization at a transmural pressure of ~10 mmHg or, as shown in Fig. 1, top, slightly > 2.40 μm. At the lower end of the normal range, the pericardial effect is reduced.[23] If we assume that the pericardium accounts for ~1 mmHg of pressure at intra-cavitary pressure 5 mmHg, the low end of the normal SL range would occur at a transmural pressure of 4 mmHg, corresponding to a SL of ~2.32 μm. Thus, our results indicate that changes in diastolic SL over the normal FP range are modest.

As the LV was filled to pressures above normal, SL reached a maximum slightly in excess of ~2.50 μm. Pressurization of the coronary bed resulted in "turgor",[14] manifested by an increase in FP. (Although the FP-SL curves with and without pressurization did not differ statistically, we believe this was due to the small number of data points.) The relation between normalized diastolic segment length and SL was unaffected by coronary pressurization. Thus, physiologic perfusion resulted in a predominantly radial as opposed to a circumferentially oriented stress on the myofibers, consistent with previous work.[24]

Our SLs are longer than those reported by Sonnenblick et al[25] in their study of anterior, midwall SLs in the normal canine LV. They also employed KCL arrest followed by glutaraldehyde fixation and measured SLs at FPs between 2 and 12 mmHg (in addition to overfilled conditions). In their report, a SL averaging2.07 μm was present at transmural pressure ~8 mmHg. With overfilling above the normal range SL reached a maximum value of ~2.25 μm. However, Sonnenblick at al[25] did not attempt to identify SL at 0 mmHg transmural pressure nor did they systematically analyze the relation between SL and FP over the normal range. One explanation for this difference in results is that Sonnenblick et al[25] did not simulate physiologic coronary perfusion. However, our finding that the normalized diastolic segment length-SL relation is unaffected by coronary pressurization makes this unlikely. Another possibility is that the EDP-SL relation differs substantially in canine and miniswine LVs. While this seems unlikely, we cannot exclude it. We believe the most likely explanation is tissue shrinkage. This may have occurred as a result of the EM methods employed by Sonnenblick et al[25], which can result in ~10% reduction in SL.[26] After fixing the tissue in situ, a procedure that by itself does not cause shrinkage as indicated by lack of change in the distance between the crystals, we used laser diffraction to measure SL without any further tissue preparation. Our methods thus minimize the possibility of shrinkage.

Rodriguez et al[27] published the only other report relating SLs to FP in the normal LV of a large mammal (closed-chest dogs). Their measurements were made by calibrating in vitro and in vivo SLs using implanted radioopaque markers. They focused on systolic SL and did not attempt to systematically determine the relation between FP and diastolic SL. However, they did estimate SL at ~ 0 mmHg transmural pressure and found this to be 2.00 – 2.05 μm, somewhat less than our estimate. Although Sonnenblick et al[25] did not measure SL at 0 mmHg, by extrapolation their value appears to be considerably less than those reported by Rodriguez et al[27] and ourselves. Both the present study and that of Rodriguez et al[27] indicate that SL at 0 mmHg is greater than slack length (1.85–1.90 μm) measured in muscle strips or isolated cardiomyocytes. One possible explanation for this difference is that residual forces[28] present at zero distending pressure significantly lengthen SL above slack length. However, Rodriquez et al[29] showed in cross-sectional rings of LV tissue that such stresses do not affect unloaded SL. This suggests that there are residual stresses inherent to the three-dimensional architecture of the fully intact LV that influence SL at 0 transmural pressure.

Under baseline conditions in our experiments estimated minimum systolic SLs were above the ~1.85–1.90 μm slack length value. However, as volume declined during bicaval occlusion minimum SLs reached values below slack in all but one experiment. At < slack length, titin is

largely responsible for cardiomyocyte diastolic recoil. The mechanism is thought to be reverse extension of titin's extensible region during contraction below slack length.[7] Thus, our results suggest that in the intact LV titin is responsible for recoil mainly at volumes below the normal range.

To estimate systolic SLs we assumed the crystals were tethered to the myocardium and that there is a linear relation between segment length measured with the crystals and SL. This relation was "calibrated" by equating the segment length at fixation with the measured SL. We inserted the crystals into the LV anterior wall at the level of the minor axis by means of a stop that positions them at a depth very close to the middle of the wall and used external landmarks to orient them circumferentially.[15] However, it is not possible to *perfectly* position the crystals circumferentially in the midwall. To the extent that the crystals differed in depth within the wall and/or were not perfectly aligned with the fibers, our method will overestimate systolic SL as the fibers shorten along their long axis and underestimate the contribution of titin to generation of a restoring force with contraction below slack length. Although our results suggest that a titin-dependent restoring force is present in the intact LV, it is important to be cautious about extrapolating to normal conditions because, in the open-chest, anesthetized state contractility is invariably depressed and loading conditions are non-physiologic. Nonetheless, our systolic SL results are consistent with those of Rodriguez et al,[27] who estimated SLs in the 1.70 range at end-systole in their intact preparation with more physiologic loading conditions.

Titin Extension

Our previous immunolabeling studies[2,4] revealed that the segments that make up titin's spring region attain a zero end-to-end length at a SL of ~1.8 μm and that the segments are slightly extended at a SL of ~1.9 μm, approximately the SL of isolated cardiomyocytes under slack conditions. This slightly extended state in slack sarcomeres is expected from statistical polymer chain analysis which shows that the mean square end-to-end distance of a flexible chain at zero external force is not zero but is a function of the contour length of the chain multiplied by its persistence length.[30] Furthermore, in a recently developed knock-out model[31] in which the N2B element was excised (reducing the contour length of titin's extensible region by ~ 50%) slack length was reduced from ~ 1.9 to 1.85 μm, supporting the idea that titin's end-to-end length in slack cardiomyocytes is non-zero and is a function of contour length. Thus, the zero force state of wild-type titin is attained at a SL of ~1.9 μm, where the extensible region is slightly extended.

We found that in miniswine diastolic SL was in the 2.15–2.25 μm range at transmural LV FP of 0 mmHg and increased slightly greater than ~2.50 μm at maximal distension, a range over which titin develops considerable passive force.[3–5] Passive force developed by titin is a function of fractional extension of the spring region, which varies for N2B and N2BA isoforms.[4] N2B titin has a shorter contour length than N2BA titin and thus the fractional extension (end-to-end length divided by contour length) for a given sarcomere stretch will be higher in N2B than N2BA when both are present within the same sarcomere. Because it is a function of contour length (see equation 1 below), force is much higher for N2B than N2BA titin. We calculated the force-SL relations of the two titin isoforms from the extension of the N2B-Us segment measured in miniswine LV (Fig. 4C). Although other segments could be used for such a calculation it is convenient to focus on N2B-Us because its large size results in the most pronounced isoform-dependent differences in extension and its persistence length is well established. Linear fits to the measured end-to-end length of N2B-Us were used to calculate the force-SL relation of single N2B and N2BA molecules, using the wormlike chain equation[2]

$$\frac{Fx(PL)}{k_B T} = \frac{z}{L} + \frac{1}{4(1 - z/L)^2} - \frac{1}{4}, \quad (1)$$

where F = force (in pN), k_B = Boltzmann's constant, T = absolute temperature, PL and L = persistence and contour lengths. With assumed PL 0.65 nm and L 210 nm^2 the predicted titin force increases much more steeply with SL for N2B than N2BA titin (Fig. 5).

As segments within titin's extensible region are in series and thus experience identical forces, the force-SL relations in Fig. 5 reflect the difference between N2B and N2BA titin molecules. Miniswine co-express N2B and N2BA at roughly similar levels and thus the resulting titin force will be intermediate between that of the two isoforms and lower than that of rodents expressing high levels of N2B titin. The working diastolic SL range of mouse LV has recently been estimated to be 1.9– 2.1 μm[32], considerably less than what we observed in miniswine. These observations combined with our own suggest that co-expression of the two isoforms in large mammals serves an important physiologic purpose. Greater expression of N2BA titin decreases the steepness of the force-SL relation, making it possible to achieve longer operating SLs without developing excessive tension and pressure. Put another way, for miniswine to operate in the range of diastolic volume and SL they do, titin isoform distribution must differ in a way that decreases stiffness.

In summary, our results indicate that in miniswine, diastolic SLs range from 2.15–2.25 to ~2.50 μm at transumural LV FPs between 0 mmHg and overfilled conditions. Over the normal operating transmural EDP range, SLs extend from ~2.32 to ~2.40 μm. Based on the observed extension of titin over these ranges, the presence of substantial amounts of N2BA titin prevents excessive diastolic pressure elevation in miniswine and, presumably, other large mammals. These results are relevant to the effects of titin isoform shifting on diastolic stiffness in cardiomyopathy[10,11]. An increase in N2BA:N2B ratio by itself would decrease stiffness. The magnitude of this effect will depend on the relation between SL and FP and the operating SL range. In a follow-on study to their original report, Ross et al[33] measured SLs in the arteriovenous fistula model of high output failure with chronic cardiac dilation. They found that operating SL range in failing animals was similar to normal, i.e., SLs were not overstretched. This result suggests that a change in titin isoforms would have the same effect on myocardial stiffness in the chronically dilated as in the normal LV

Acknowledgments

Funding Sources

Research supported by NIH grants RO1 HL61497 and HL062881.

References

1. LeWinter MM, Wu Y, Labeit S, Granzier H. Cardiac titin: structure, functions and role in disease. Clin Chim Acta 2007;375:1–9. [PubMed: 16904093]
2. Watanabe K, Nair P, Labeit D, Kellermayer MS, Greaser M, Labeit S, Granzier H. Molecular mechanics of cardiac titin's PEVK and N2B spring elements. J Biol Chem 2002;277:11549–58. [PubMed: 11799131]
3. Granzier H, Helmes M, Cazorla O, McNabb M, Labeit D, Wu Y, Yamasaki R, Redkar A, Kellermayer M, Labeit S, Trombitás K. Mechanical properties of titin isoforms. Adv Exp Med Biol 2000;481:283–300. [PubMed: 10987079]

4. Trombitás K, Redkar A, Centner T, Wu Y, Labeit S, Granzier H. Extensibility of isoforms of cardiac titin: variation in contour length of molecular subsegments provides a basis for cellular passive stiffness diversity. Biophys J 2000;79:3226–34. [PubMed: 11106626]
5. Granzier HL, Irving TC. Passive tension in cardiac muscle: contribution of collagen, titin, microtubules, and intermediate filaments. Biophys J 1995;68:1027–44. [PubMed: 7756523]
6. Wu Y, Bell SP, Trombitas K, Witt CC, Labeit S, LeWinter MM, Granzier H. Changes in titin isoform expression in pacing-induced cardiac failure give rise to increased passive muscle stiffness. Circulation 2002;106:1384–9. [PubMed: 12221057]
7. Helmes M, Trombitás K, Granzier H. Titin develops restoring force in rat cardiac myocytes. Circ Res 1996;79:619–26. [PubMed: 8781495]
8. Cazorla O, Freiburg A, Helmes M, Centner T, McNabb M, Wu Y, Trombitás K, Labeit S, Granzier H. Differential expression of cardiac titin isoforms and modulation of cellular stiffness. Circ Res 2000;86:59–67. [PubMed: 10625306]
9. Wu Y, Cazorla O, Labeit D, Labeit S, Granzier H. Changes in titin and collagen underlie diastolic stiffness diversity of cardiac muscle. J Mol Cell Cardiol 2000;32:2151–62. [PubMed: 11112991]
10. Neagoe C, Kulke M, del Monte F, Gwathmey JK, de Tombe PP, Hajjar RJ, Linke WA. Titin isoform switch in ischemic human heart disease. Circulation 2002;106:1333–41. [PubMed: 12221049]
11. Nagueh SF, Shah G, Wu Y, Torre-Amione G, King NM, Lahmers S, Witt CC, Becker K, Labeit S, Granzier HL. Altered titin expression, myocardial stiffness, and left ventricular function in patients with dilated cardiomyopathy. Circulation 2004;110:155–62. [PubMed: 15238456]
12. Trombitás K, Wu Y, Labeit D, Labeit S, Granzier H. Cardiac titin isoforms are coexpressed in the half-sarcomere and extend independently. Am J Physiol Heart Circ Physiol 2001;281:H1793–9. [PubMed: 11557573]
13. Zile MR, Baicu CF, Gaasch WH. Diastolic heart failure--abnormalities in active relaxation and passive stiffness of the left ventricle. N Engl J Med 2004;350:1953–9. [PubMed: 15128895]
14. Wyman RM, Farhi ER, Bing OH, Johnson RG, Weintraub RM, Grossman W. Comparative effects of hypoxia and ischemia in the isolated, blood-perfused dog heart: evaluation of left ventricular diastolic chamber distensibility and wall thickness. Circ Res 1989;64:121–8. [PubMed: 2909295]
15. LeWinter MM, Kent RS, Kroener JM, Carew TE, Covell JW. Regional differences in myocardial performance in the left ventricle of the dog. Circ Res 1975;37:191–9. [PubMed: 1149193]
16. Streeter DD Jr, Spotnitz HM, Patel DP, Ross J Jr, Sonnenblick EH. Fiber orientation in the canine left ventricle during diastole and systole. Circ Res 1969;24:339–47. [PubMed: 5766515]
17. Ross MA, Streeter DD Jr. Nonuniform subendocardial fiber orientation in the normal macaque left ventricle. Eur J Cardiol 1975;3:229–47. [PubMed: 810355]
18. Wickline SA, Verdonk ED, Miller JG. Three-dimensional characterization of human ventricular myofiber architecture by ultrasonic backscatter. J Clin Invest 1991;88:438–46. [PubMed: 1864957]
19. Geerts L, Bovendeerd P, Nicolay K, Arts T. Characterization of the normal cardiac myofiber field in goat measured with MR-diffusion tensor imaging. Am J Physiol Heart Circ Physiol 2002;283:H139–45. [PubMed: 12063284]
20. Ennis DB, Nguyen TC, Riboh JC, Wigström L, Harrington KB, Daughters GT, Ingels NB, Miller DC. Myofiber angle distributions in the ovine left ventricle do not conform to computationally optimized predictions. J Biomech 2008;41:3219–24. [PubMed: 18805536]
21. Wu Y, Tobias AH, Bell K, Barry W, Helmes M, Trombitas K, Tucker R. Campbell Cellular and molecular mechanisms of systolic and diastolic dysfunction in an avian model of dilated cardiomyopathy. J Mol Cell Cardiol 2004;37:111–9. [PubMed: 15242741]
22. Snedecor, GW.; Cochran, WG. Statistical Methods. 6. The Iowa State University Press; Ames, Iowa: 1967.
23. Slinker BK, Ditchey RV, Bell SP, LeWinter MM. Right heart pressure does not equal pericardial pressure in the potassium chloride-arrested canine heart in situ. Circulation 1987;76:357–62. [PubMed: 3608123]
24. May-Newman K, Omens JH, Pavelec RS, McCulloch AD. Three-dimensional transmural mechanical interaction between the coronary vasculature and passive myocardium in the dog. Circ Res 1994;74:1166–78. [PubMed: 8187283]

25. Sonnenblick EH, Ross J Jr, Covell JW, Spotnitz HM, Spiro D. The ultrastructure of the heart in systole and diastole: Changes in sarcomere length. Circ Res 1967;21:423–431. [PubMed: 6057700]

26. Granzier HL, Akster HA, Ter Keurs HE. Effect of thin filament length on the force- sarcomere length relation of skeletal muscle. Am J Physiol 1991;260:C1060–70. [PubMed: 2035614]

27. Rodriguez EK, Hunter WC, Royce MJ, Leppo MK, Douglas AS, Weisman HF. A method to reconstruct myocardial sarcomere lengths and orientations at transmural sites in beating canine hearts. Am J Physiol 1992;263:H293–306. [PubMed: 1636767]

28. Omens JH, Rockman HA, Covell JW. Passive ventricular mechanics in tight-skin mice. Am J Physiol 1994;266:H1169–76. [PubMed: 8160820]

29. Rodriguez EK, Omens JH, Waldman LK, McCulloch AD. Effect of residual stress on transmural sarcomere length distributions in rat left ventricle. Am J Physiol 1993;264:H1048–56. [PubMed: 8476082]

30. Rivetti C, Guthold M, Bustamante C. Scanning force microscopy of DNA deposited onto mica: equilibration versus kinetic trapping studied by statistical polymer chain analysis. J Mol Biol 1996;264:919–32. [PubMed: 9000621]

31. Radke MH, Peng J, Wu Y, McNabb M, Nelson OL, Granzier H, Gotthardt M. Targeted deletion of titin N2B region leads to diastolic dysfunction and cardiac atrophy. Proc Natl Acad Sci U S A 2007;104:3444–9. [PubMed: 17360664]

32. Toh R, Shinohara M, Takaya T, Yamashita T, Masuda S, Kawashima S, Yokoyama M, Yagi N. An X-ray diffraction study on mouse cardiac cross-bridge function in vivo: effects of adrenergic β-stimulation. Biophysical Journal 2006;90:1723–28. [PubMed: 16339874]

33. Ross J Jr, Sonnenblick EH, Taylor RR, Spotnitz HM, Covell JW. Diastolic geometry and sarcomere lengths in the chronically dilated canine left ventricle. Circ Res 1971;28:49–61. [PubMed: 5539440]

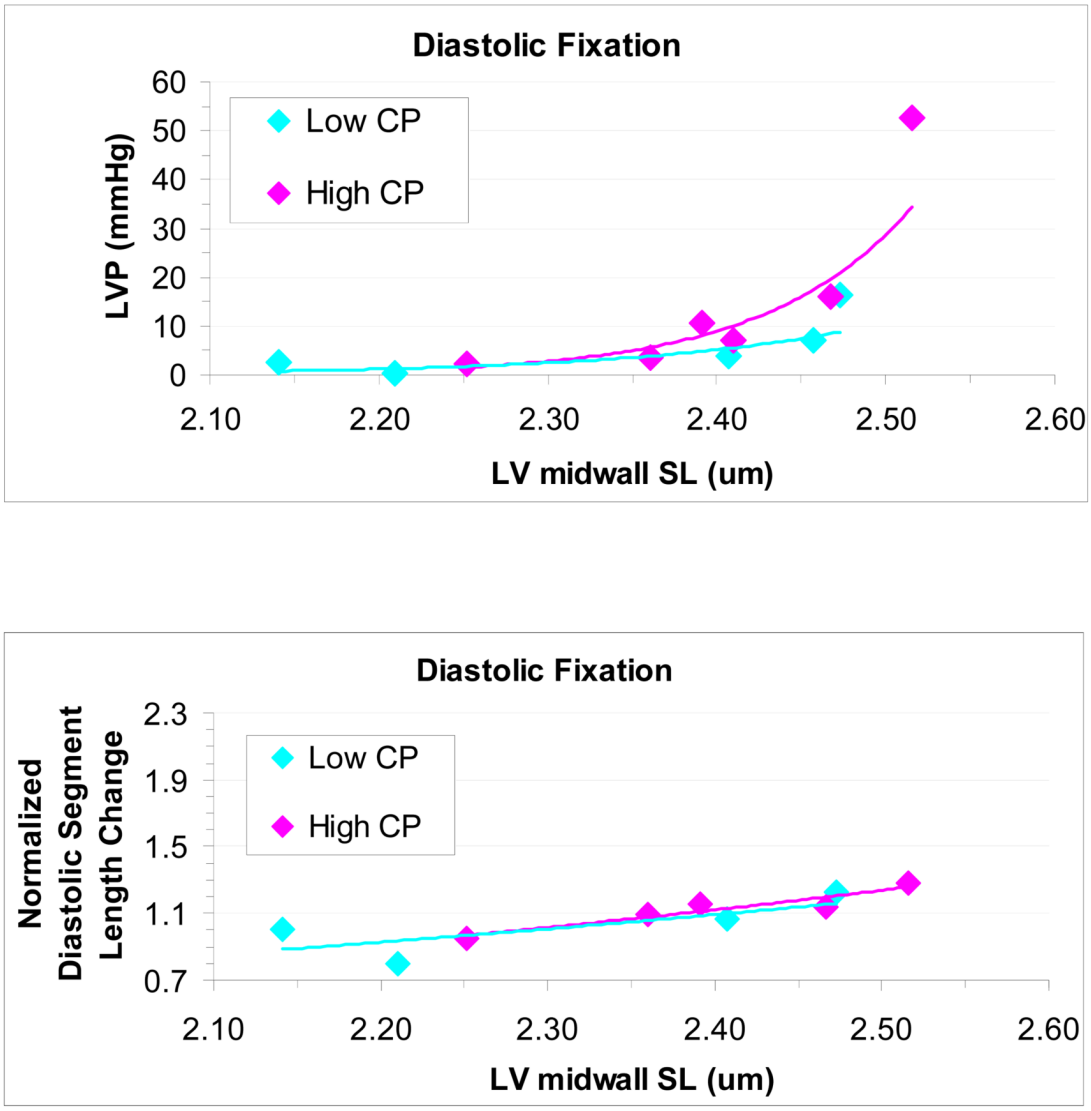

Figure 1.
Top, filling pressure-SL relations in arrested LV with and without physiologic coronary perfusion pressure. Bottom, normalized diastolic segment length change-SL relations. See text for details.

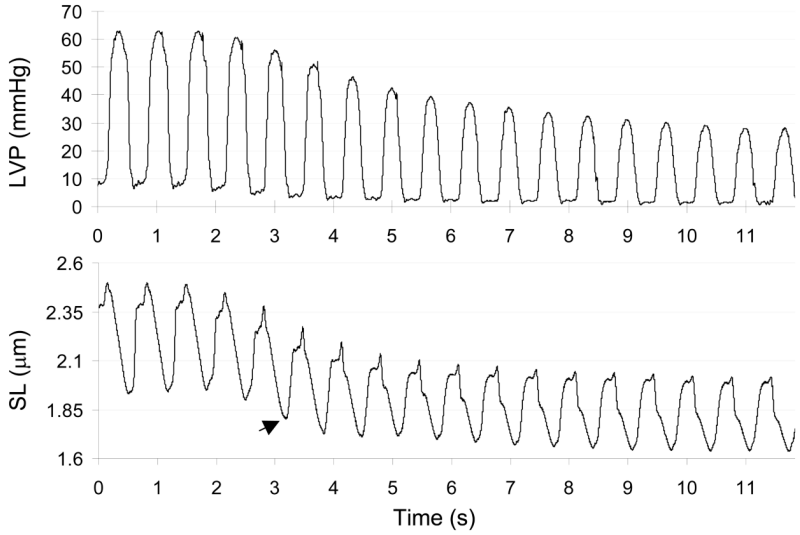

Figure 2.
An example of LV pressure and segment length during bicaval occlusion. Segment length converted to SL. See text for details.

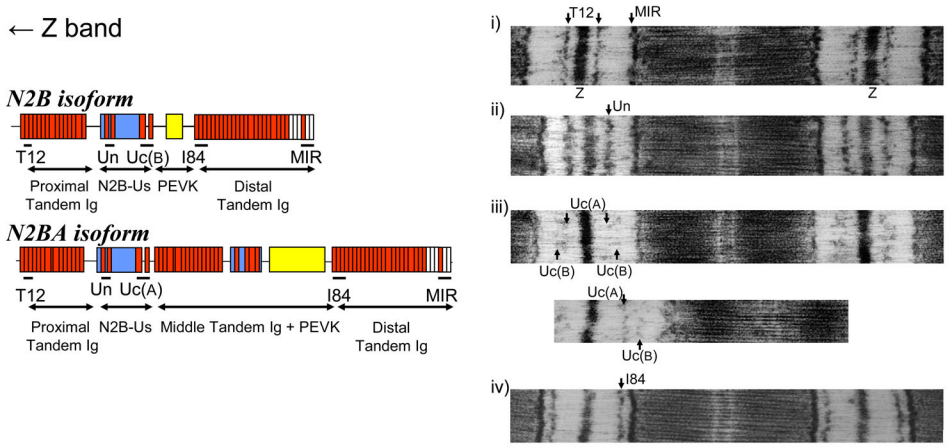

Figure 3.

Left, domain structure of extensible I-band region of cardiac N2B (top) and N2BA (bottom) isoforms. Red: Ig domains; blue: unique sequences; yellow: PEVK sequence; white: fibronectin domains. Antibodies used were raised against epitopes indicated by horizontal lines. T12 is directed to I2/I3; UN to I24/I25; UC to I26/I27, I84 to I84–I86, MIR: I109 –I111. These antibodies mark the proximal and distal tandem Ig segments, the N2B unique sequence (N2B-Us), PEVK (N2B isoform) and PEVK plus middle tandem Ig (N2BA isoform). Right, examples of sarcomeres labeled with anti-titin antibodies. All sarcomeres are labeled with MIR (except for bottom micrograph of iii)) and one additional antibody. Note from iii) that Uc labels two epitopes, best seen in the bottom micrograph. This has been studied in other species that co-express titin isoforms and is due to the extra extensibility of the middle tandem Ig and PEVK of N2BA titin. As a result the UC epitope of N2BA titin [named UC(A)] is closer to the Z-line than the UC epitope of N2B titin [UC(B)]. (For details, see Trombitas et al.[12]).

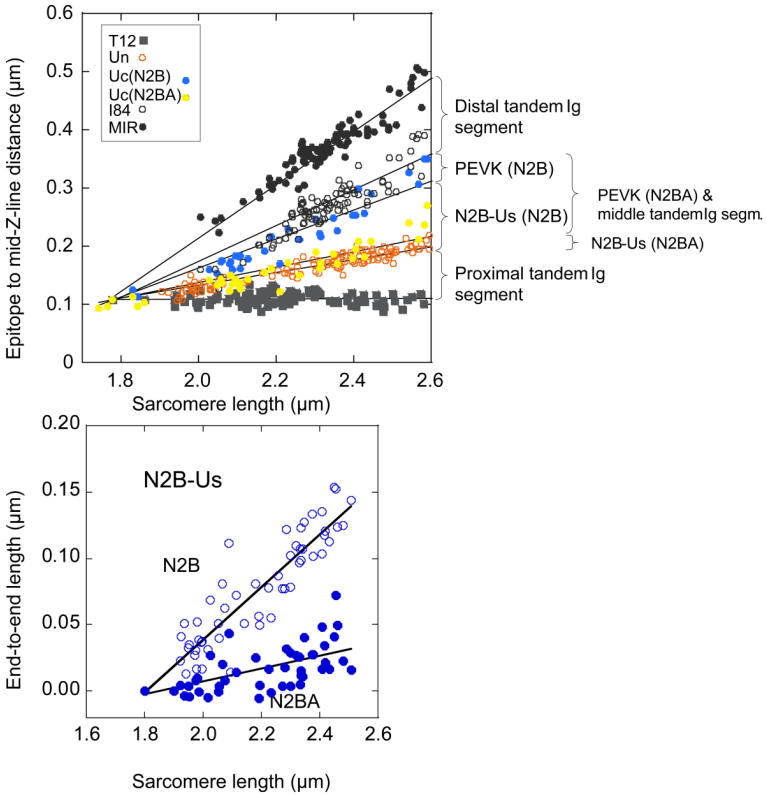

Figure 4.

Top, scattergram of epitope to Z-line distance vs. SL. Labeling patterns are assumed to be derived from co-expressed N2B and N2BA isoforms. The lengths of the various I-band segments were determined as shown in the left side of Figure 3. Bottom, lengths of N2B-Us for N2B and N2BA isoforms. The large number of data points reflect the fact that approximately 10 strips were available per heart.

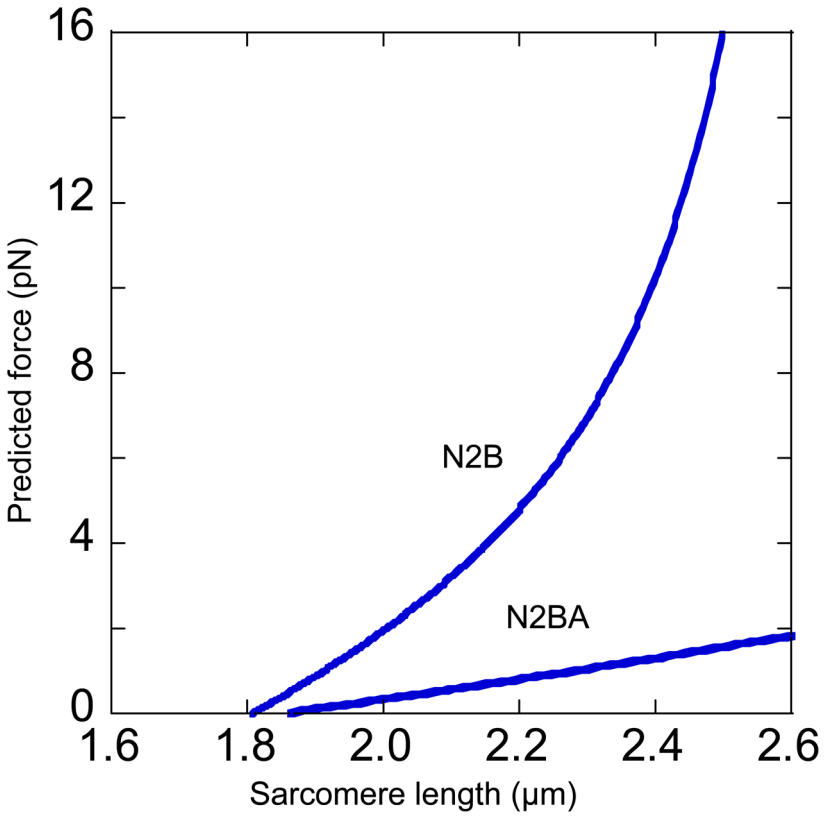

Figure 5.
Predicted force-SL relation of N2B and N2BA titin based on measured length of N2B-Us (Bottom, Fig. 4C) (see text for details).